Consequences of imperfect mixing the Gray-Scott model

M.-P. Zorzano,[1,*] D. Hochberg,[1,†] and F. Morán[1,2,‡]
[1]*Centro de Astrobiología (CSIC-INTA), Carretera de Ajalvir km 4, 28850 Torrejón de Ardoz, Madrid, Spain*
[2]*Departamento de Bioquímica y Biología Molecular, Facultad de Ciencias Químicas, Universidad Complutense de Madrid, Spain*
(Received 8 May 2006; revised manuscript received 26 September 2006; published 16 November 2006)

We study an autocatalytic reaction-diffusion scheme, the Gray-Scott model, when the mixing processes do not homogenize the reactants. Starting from the master equation, we derive the resulting coupled, nonlinear, stochastic partial differential equations that rigorously include the spatiotemporal fluctuations resulting from the interplay between the reaction and mixing processes. The fields are complex and depend on correlated complex noise terms. We implement a method to solve for these complex fields numerically and extract accurate information about the system evolution and stationary states under different mixing regimes. Through this example, we show how the reaction-induced fluctuations interact with the temporal nonlinearities, leading to results that differ significantly from the mean-field (perfectly mixed) approach. This procedure can be applied to an arbitrary nonlinear reaction diffusion scheme.

DOI: 10.1103/PhysRevE.74.057102 PACS number(s): 82.40.Ck, 05.10.Cc, 05.40.Ca, 89.75.Kd

Reaction diffusion networks are relevant to a broad scope of chemical, biological, and nonlinear optical systems where the agents must diffuse about before they meet and react [1]. To date, much of the theoretical work devoted to the analysis of reaction network dynamics has been based on the assumption that the system is "well mixed," i.e., that the concentration of each species is always uniform throughout the system. This regime is then solved using mean-field approximations, which may be adequate under perfect stirring conditions or equivalently when the diffusion rates are very high. But if the reaction rates are nonlinear, which is the case of the ubiquitous autocatalytic and catalytic networks, any departure from the assumption of perfect mixing can have major dynamical consequences. There are numerous experimental evidences on the outcome of catalytic processes under imperfect mixing [2]. For instance, it has been experimentally shown that imperfect mixing in autocatalytic systems can lead to chemical reactions that occur at seemingly random intervals [3], crystallization processes that yield sometimes all left-handed and sometimes all right-handed crystals [4], and reactions in which changing the rate at which a solution is stirred can cause a transition from a stationary, time-independent state to one of periodic, or even chaotic oscillation [5]. These phenomena have been studied primarily in inorganic chemical media, but there are implications also for relevant biological systems: hypercycle networks, viral quasispecies dynamics, ecosystems, etc. [6–8]. There is a wealth of theoretical works related to the effects of fluctuations on these systems that intuitively show the relevance that density fluctuations may have on stability, pattern formation, and the effects of dimensionality [9]. However, in these approaches, the fluctuations are simply added *ad hoc* to the mean-field description and the noise strength and correlations are chosen arbitrarily.

In this Brief Report, we address this issue and work through a general-purpose, mathematical, and numerical procedure to study the mixing process in reaction-diffusion problems. The mixing process in nonlinear reaction systems has been described mostly for simple reaction schemes [10] but has not been fully exploited to solve for the Langevin-type equation, since the fluctuations in the general case turn out to be complex. Our approach is based on (i) the application of a standard, field-theoretic method to characterize the reaction-induced fluctuations and derive a Langevin-type description of the underlying molecular dynamics; (ii) the nondimensionalization of the problem to characterize the dependence on the agents' diffusivities, reaction rates, and the spatial dimension; and (3) the separation of the real and imaginary parts of the noise to solve numerically for the real and imaginary parts of the stochastic fields. As an example of this consistent description, we treat the Gray-Scott (GS) model in two spatial dimensions [11] and *vary the diffusion rates to rigorously explore different mixing regimes*. We choose this model to facilitate visualizing the differences between perfect and imperfect mixing because the GS model is known to exhibit spatial pattern formation and to be very sensitive to multiplicative noise [12]. This procedure can be applied to an arbitrary reaction scheme for any spatial dimension. The method presented here allows one to solve for the *full set of complex Langevin equations* and to extract information about the spatiotemporal time evolution of the system and its stationary states under different mixing regimes. We show numerically that only the noise averaged real parts of the complex fields correspond to the density of the reactants. We compare our results to the mean-field case, which is recovered only in the infinite diffusion limit.

The GS model, corresponds to the following chemical reactions:

$$U + 2V \xrightarrow{\lambda} 3V,$$

$$V \xrightarrow{\mu} p,$$

$$U \xrightarrow{\nu} q,$$

*Electronic address: zorzanomm@inta.es; URL: http://www.cab.inta.es
†Electronic address: hochberg@laeff.esa.es
‡Electronic address: fmoran@solea.quim.ucm.es

$$\overset{u_0}{\rightarrow} U. \tag{1}$$

The concentrations of the chemical species V and U are functions of d-dimensional space $\vec{x}$ and time t. λ is the reaction rate, p and q are inert products, μ is the decay rate of V, and ν is the decay rate of U. The equilibrium concentration of b is u_0/ν, where u_0 is the feed rate constant. The chemical species U and V can diffuse with independent diffusion constants D_u and D_v. All the model parameters are positive.

The master equation associated with Eq. (1) can be mapped to a second-quantized description following a procedure developed by Doi [13]. Briefly, we introduce annihilation and creation operators a_i and $a_i^\dagger$ for V and b_i and $b_i^\dagger$ for U at each lattice site i, with the commutation relations $[a_i, a_j^\dagger] = \delta_{ij}$ and $[b_i, b_j^\dagger] = \delta_{ij}$. The vacuum state satisfies $a_i|0\rangle = b_i|0\rangle = 0$. We then define the time-dependent state vector $|\Psi(t)\rangle = \Sigma_{\{m\},\{n\}} P(\{m\},\{n\},t) \Pi_i (a_i^\dagger)^{m_i} (b_i^\dagger)^{n_i} |0\rangle$. $P(\{m\},\{n\},t)$ is the probability to find m_i U and n_i V particles at site i at time t. The master equation can be written as a Schrödinger-like equation $-\frac{\partial|\Psi(t)\rangle}{\partial t} = H|\Psi(t)\rangle$, where the lattice Hamiltonian or time-evolution operator is a function of $a_i, a_i^\dagger, b_i, b_i^\dagger$ and is given by

$$\begin{aligned} H = {} & \frac{D_v}{l^2} \sum_{(i,j)} (a_i^\dagger - a_j^\dagger)(a_i - a_j) + u_0 \sum_i (1 - b_i^\dagger) + \frac{D_u}{l^2} \sum_{(i,j)} (b_i^\dagger - b_j^\dagger) \\ & \times (b_i - b_j) - \frac{\lambda}{2} \sum_i [(a_i^\dagger)^3 a_i^2 b_i - (a_i^\dagger)^2 a_i^2 b_i^\dagger b_i] \\ & + \nu \sum_i (b_i^\dagger - 1) b_i + \mu \sum_i (a_i^\dagger - 1) a_i. \end{aligned} \tag{2}$$

This has the formal solution $|\Psi(t)\rangle = \exp(-Ht)|\Psi(0)\rangle$.

The operator [Eq. (2)] is next mapped onto a continuum field theory. This procedure is now standard, and we refer to [14] for further details. For the GS system, we obtain the path integral $\exp(-Ht) = \int \mathcal{D}a \mathcal{D}\bar{a} \mathcal{D}b \mathcal{D}\bar{b} e^{-S[a,\bar{a},b,\bar{b}]}$, over the continuous (and generally complex) stochastic fields $a(\vec{x},t), \bar{a}(\vec{x},t), b(\vec{x},t), \bar{b}(\vec{x},t)$, where the action S is given by

$$\begin{aligned} S = \int d^d x \int_0^\tau dt \Big[& \bar{a}\partial_t a + D_v \nabla \bar{a} \nabla a + \bar{b}\partial_t b + D_u \nabla \bar{b} \nabla b + \mu(\bar{a} \\ & - 1)a + \nu(\bar{b} - 1)b - u_0(\bar{b} - 1) - \frac{\lambda}{2}(\bar{a}^3 a^2 b - \bar{a}^2 a^2 \bar{b} b) \Big]. \end{aligned} \tag{3}$$

We have omitted terms related to the initial state. Apart from taking the continuum limit, the derivation of this action is exact and, in particular, no assumptions regarding the precise form of the noise are required. For the final step, we perform the shift $\bar{a} = 1 + a^*$ and $\bar{b} = 1 + b^*$ on the action S. We represent the terms quadratic in a^*, b^* by an integration over Gaussian noise terms, which allows us to then integrate out the conjugate fields [19]. To proceed, we note that $e^{\lambda a^2 b (a^{*2} - a^* b^*)} \approx \int \mathcal{D}\xi \mathcal{D}\eta P(\xi,\eta)\, e^{(a^*\xi + b^*\eta)}$, where the noise functions ξ, η are distributed according to a double Gaussian as $P(\xi,\eta) = \exp\left[-(\xi,\eta) V^{-1} \binom{\xi}{\eta}\right]$, with V the matrix of noise-noise correlation functions

$$V = \begin{pmatrix} \langle \xi\xi \rangle & \langle \eta\xi \rangle \\ \langle \xi\eta \rangle & \langle \eta\eta \rangle \end{pmatrix}. \tag{4}$$

Integrating out the conjugate fields a^* and b^* from the functional integral for this shifted action then leads to the pair of coupled nonlinear Langevin equations. We define the dimensionless fields, $u = \frac{\lambda}{\mu} b$ and $v = \frac{\lambda}{\mu} a$, dimensionless time, $\tau = \mu t$, and spatial coordinates $x_i = \sqrt{\mu/D_u}\, \hat{x}_i$, $i = 1, \ldots, d$. The equations describing the field dynamics read

$$\begin{aligned} \partial_\tau v(\hat{x}_i,\tau) &= \frac{D_v}{D_u} \nabla^2 v - v + v^2 u + \xi(\hat{x}_i,\tau) \\ \partial_\tau u(\hat{x}_i,\tau) &= \nabla^2 u - \frac{\nu}{\mu} u - v^2 u + \frac{u_0}{\mu} + \eta(\hat{x}_i,\tau), \end{aligned} \tag{5}$$

with noise correlations

$$\begin{aligned} \langle \xi(\hat{x}_i,\tau) \rangle &= \langle \eta(\hat{x}_i,\tau) \rangle = 0 \\ \langle \xi(\hat{x}_i,\tau) \xi(\hat{x}_i',\tau') \rangle &= \epsilon v^2 u \delta^2(\hat{x}_i - \hat{x}_i') \delta(\tau - \tau') \\ \langle \xi(\hat{x}_i,\tau) \eta(\hat{x}_i',\tau') \rangle &= -\frac{\epsilon}{2} v^2 u \delta(\hat{x}_i - \hat{x}_i') \delta(\tau - \tau') \\ \langle \eta(\hat{x}_i,\tau) \eta(\hat{x}_i',\tau') \rangle &= 0, \end{aligned} \tag{6}$$

and noise strength $\epsilon = \sqrt{\lambda} \frac{\mu^{(d-1)/2}}{D_u^{d/2}}$. In particular, for $d=2$ dimensions, $\epsilon = \frac{\sqrt{\lambda\mu}}{D_u}$. The nondimensionalization of the problem allows us to characterize explicitly the dependence on the agents diffusivities, reaction rates, and spatial dimension. For a fixed reaction rate, as we will see below, the transition from perfect to the imperfect mixing regime is associated with an increase in ϵ. Note that η has zero autocorrelation but nonzero cross-correlation with ξ, indicating that this noise is *complex*. Using the Cholesky decomposition, we can express these complex noise components as a linear combination of two uncorrelated (real) white Gaussian noises θ_1, θ_2; thus,

$$\xi(\hat{x}_i;\tau) = v\sqrt{\epsilon u}\, \theta_1(\hat{x}_i;\tau) \tag{7}$$

$$\eta(\hat{x}_i;\tau) = -\tfrac{1}{2} v \sqrt{\epsilon u}\, \theta_1(\hat{x}_i;\tau) + i \tfrac{1}{2} v \sqrt{\epsilon u}\, \theta_2(\hat{x}_i;\tau). \tag{8}$$

Thus, u and v are also complex fields. Through this procedure we can separate the real and imaginary parts of the noise and numerically solve the stochastic nonlinear reaction diffusion equations (5) for the real and imaginary parts of the fields [15]. Now we can obtain numerical information from these complex densities. We expect the imaginary parts of these fields to be zero, on average, since the stochastic averages $\langle u \rangle$ and $\langle v \rangle$ correspond to the physical reactant densities [16].

In the mean-field approximation, this system possesses three homogeneous solutions: one absorbing state $R = \left(u = \frac{u_o}{\nu}\frac{\lambda}{\mu}, v = 0\right)$ and two nontrivial states $B_\pm = \left(u = \frac{u_o \pm \sqrt{u_o^2 - 4\nu\mu^2/\lambda}}{2\nu}\frac{\lambda}{\mu}, v = \frac{1}{u}\frac{\lambda}{\mu}\right)$. In our simulations, we consider the $d=2$ case with $\lambda = 1$, $D_v/D_u = 0.5$, $u_o = \nu$ and, thus, the homogeneous solutions will be $R = \left(u = \frac{1}{\mu}, v = 0\right)$ and

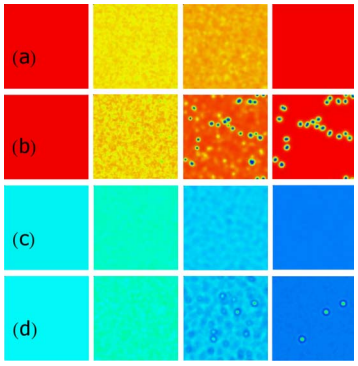

FIG. 1. (Color online) Each row of squares shows, from left to right, the time evolution of Re $u(\hat{x},\hat{y},\tau)$ for a different simulation. The initial condition, at $\tau=0$, is shown on the leftmost image, see text for details. (a) and (b) have the same initial condition and reaction parameters. (a) If $\epsilon\to 0$, which corresponds to the *perfect mixing regime*, then the system evolves to the uniform absorbing state R (here shown at $\tau=50$). (b) As ϵ increases, in the *imperfect mixing regime*, the system evolves to a *new* active state with globular replicating structures ($\tau=50$). Equivalently, for a new initial condition and parameter set, (c) evolves in the *perfect mixing regime* to the uniform active state B_- ($\tau=300$), whereas (d), in the *imperfect mixing regime*, evolves to a *new* active state ($\tau=300$).

$B_\pm=\left(u=\frac{1\pm\sqrt{1-4\mu^2/\nu}}{2}\frac{1}{\mu}, v=\frac{1}{u}\frac{1}{\mu}\right)$. The state B_+ is globally unstable. The trivial state R is linearly stable and globally attracting for all $\nu>0$ and $\mu>\nu$. The state B_- is stable if $4\mu^2>\nu$. In a narrow region of parameter space (μ,ν) close to $4\mu^2=\nu$, the trivial absorbing state R loses stability through a Hopf bifurcation. In the *noise-free* case, it is in the vicinity of this region where one can find a great variety of spatiotemporal patterns in response to a localized initial spatial perturbation [17], although no patterns are found if the initial condition is homogeneous. Here we will consider the evolution of the system described by Eqs. (5) with initial *homogeneous condition* and subject to the internal noise induced by the reaction [Eqs. (7) and (8)] in different mixing regimes.

In Fig. 1, we display some "snapshots" of the time evolution of the real part of the nutrient field $u(\hat{x},\hat{y},t)$ for two different parameter sets and two diffusion rates. When displayed in color, blue represents a concentration between $\frac{0.2}{\mu}$ and $\frac{0.4}{\mu}$, green close to $\frac{0.5}{\mu}$, yellow represents an intermediate concentration of roughly $\frac{0.8}{\mu}$, and red close to $\frac{1}{\mu}$. On a gray scale, lighter grays correspond to low concentration and darker ones to high concentration. Figures 1(a) and 1(b) represent the time evolution of the same initial homogeneous condition $\left(u=\frac{1}{\mu}, v=\frac{0.1}{\mu}\right)$ for $\mu=0.095$ and $\nu=0.03$. In Fig. 1(a), a regime of high diffusion rates ($\epsilon=0.01225$), initially there are some local spatial fluctuations about the mean value. Then, the fluctuations are homogenized due to the high diffusivity of the reactants and the system evolves toward the inactive homogeneous state R of the mean-field approach. This is the result we may expect in a perfect mixing regime. In Fig. 1(b), we have increased the noise strength ($\epsilon=0.0225$) by reducing the diffusion rates (i.e., to explore deviations from the mean-field results we allow for the imperfect mixing effects): the strong spatial incoherent fluctuations give rise to spatial patterns with self-replicating and moving globules. In the interior of each of these units, in blue, there is a region with sustained autocatalytic production of v that is causing the local depletion of the substrate u. A similar experiment is shown in Figs. 1(c) and 1(d), with a new initial condition $\left(u=\frac{0.5}{\mu}, v=\frac{0.25}{\mu}\right)$, and parameter set $\mu=0.11025$, $\nu=0.05$. The initial condition is again the same in both cases, but in the perfect mixing regime where the system has a high diffusion rate (and a low noise intensity, such as $\epsilon=0.01$), it evolves to the uniform stable active state B_- [see Fig. 1(c)], whereas in the imperfect mixing regime with low diffusion rates (and higher noise intensities, such as $\epsilon=0.023$), the system evolves to a new active pattern with globular structures. Thus, in Figs. 1(b)–1(d), a low diffusion rate has induced fluctuations that drive the system away from the absorbing state R or the uniform blue state B_- and produces spatial compartmentalization.

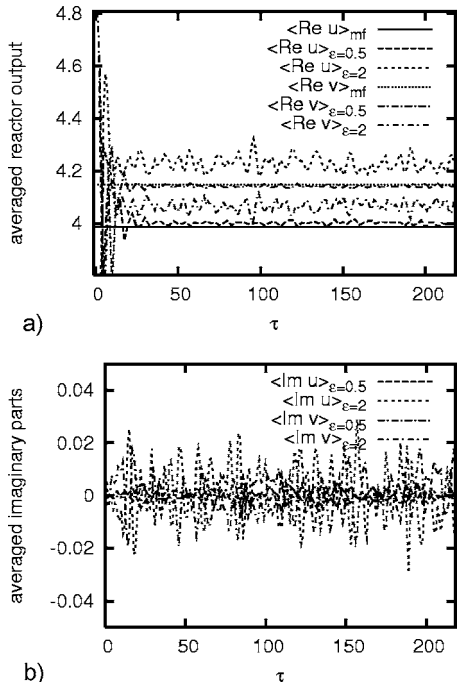

FIG. 2. (a) After a transient time, in the perfect mixing limit $\epsilon=0.5$, the average of the real part of the field tends to the mean-field value. However, in the imperfect mixing regime, $\epsilon=2$, these averages deviate significantly from the mean-field solution and show oscillatory behavior. (b) The averaged imaginary parts of the fields are always negligible since the averages correspond to physical, real, densities.

Because of the imperfect mixing effects, the averaged output of the reactor (integrated over $\hat{x}$ and $\hat{y}$) may also change with the diffusion rate. In Fig. 2 (a), we show, for $\mu=0.0605$, $\nu=0.02$ and starting with the initial homogeneous condition $\left(u=\frac{0.3}{\mu}, v=\frac{0.25}{\mu}\right)$, how for the average of the real part of the field, which corresponds to the density, different mixing regimes lead to different reactor outputs. For very high diffusion rates (and low noise intensities ϵ), the system evolves to the mean-field solution $(\langle \mathrm{Re}\, u\rangle_{mf}, \langle \mathrm{Re}\, v\rangle_{mf})=B_-$, note that $\langle \mathrm{Re}\, v\rangle > \langle \mathrm{Re}\, u\rangle$. If the diffusivity of reactants is reduced, the system evolves to a new equilibrium state with the reversed ratio $\langle \mathrm{Re}\, v\rangle < \langle \mathrm{Re}\, u\rangle$. Furthermore, after the initial transient time, the output of the reactor shows *oscillatory*

behavior, which increases in amplitude as we deviate from the perfect mixing regime. In Fig. 2 (b), we show for the same simulations the average of the imaginary part of the field, confirming that the averaged imaginary part is zero up to the statistical error.

Thus, in any system governed by a nonlinear rate law, a knowledge of the bulk or average concentrations is not sufficient to predict either the average rate of the reaction, the final equilibrium spatial distribution, or the averaged reactor output. One must also know the spatial distribution of the reacting material. Furthermore, there is a strong dependence on the ratio of the reaction to diffusion rate and the mean-field approach will only be valid in the limit where this ratio vanishes. The noise parameter ϵ is a function of the spatial dimensionality, suggesting that the resulting rates of reaction, spatial distribution, and global-averaged densities of reactants may change from two to three dimensions and the simple extrapolation of two-dimensional model results may not be adequate. Finally, these results show that one can thus tune the mixing efficiently to control the composition of the output of the reactor and, second, that for certain ranges of diffusion rates we may discover unexplored dynamical ranges where spatial organization takes place. One may also appreciate the relevance that the mixing process will have in biological systems, such as epidemics propagation or in viral dynamics [18], where spatial segregation may facilitate coexistence.

This general-purpose, consistent mathematical, and numerical approach allows us to rigorously explore the effects of reaction-induced fluctuations in imperfect mixing regimes with complex fields and noises. Dealing with the full system, we observe that there is multiplicative noise acting on *both* fields. If we had ignored the zero-autocorrelated complex field η in Eq. (6), then only the v field would have had noise and both field and ξ would have been real [15]. This approximation is not correct in the general case, and the system outcome may be significantly different in nonlinear systems, such as this one, which is quite sensitive to small fluctuations.

M.-P.Z. is supported by the Instituto Nacional de Técnica Aerospacial (INTA). The research of D.H. is supported in part by INTA, and F.M. is supported in part by Grant No. BMC2003-06957 from MEC (Spain).

[1] M. C. Cross and P. C. Hohenberg, Rev. Mod. Phys. **65**, 851 (1993).
[2] I. R. Epstein, Nature (London) **374**, 321 (1995).
[3] I. Nagypal and I. R. Epstein, Chem. Phys. **89**, 6925 (1988).
[4] D. K. Kondepudi, R. J. Kaufman, and N. Singh, Science **250**, 975 (1990).
[5] L. Gyorgyi, R. J. Field, Z. Noszticzius, W. D. McCormick, and H. L. Swinney, J. Phys. Chem. **96**, 1228 (1992).
[6] *Spatial Ecology via Reaction-Diffusion Equations*, edited by R. S. Cantrell and C. Cosner, Wiley Series on Mathematical and Computational Biology (John Wiley and Sons, Chichester, Sussex UK, 2003).
[7] C. O. Wilke, J. L. Wang, C. Ofria, R. E. Lenski, and C. Adami, Nature (London) **412**, 333 (2001).
[8] K. M. Cuddington and P. Yodzis, Theor Popul. Biol. **58**, 259 (2000).
[9] J. García-Ojalvo and J. M. Sancho, *Noise in Spatially Extended Systems* (Springer-Verlag, Berlin, 1999).
[10] D. Toussaint and F. Wilczek, J. Phys. Chem. **78**, 2643 (1983).
[11] P. Gray and S. K. Scott, Chem. Eng. Sci. **38**, 29 (1983); P. Gray and S. K. Scott, *ibid.* **39**, 1087 (1984); **89**, 22 (1985).
[12] D. Hochberg, M.-P. Zorzano, and F. Morán, J. Phys. Chem. **122**, 214701 (2005).
[13] M. Doi, J. Phys. A **9**, 1465 (1976).
[14] L. Peliti, J. Phys. (Paris) **46**, 1469 (1985).
[15] D. Hochberg, M.-P. Zorzano, and F. Morán, Chem. Phys. Lett. **426**, 54 (2006).
[16] M. J. Howard and U. C. Täuber, J. Phys. A **30**, 7721 (1997).
[17] J. E. Pearson, Science **261**, 189 (1993).
[18] C. K. Biebricher and M. Eigen, Curr. Top. Microbiol. Immunol. **299**, 1 (2006).
[19] This can be done provided we ignore the cubic terms, which would give information on higher-order cumulants of the fluctuations.